Astron. Astrophys. 217, 57–65 (1989)

ASTRONOMY AND ASTROPHYSICS

A comparative study of Na I and Ca II infrared lines in stars, star clusters and galaxy nuclei: an alternative to the dwarf-enriched population

D. Alloin[1] and E. Bica[2]

[1] DAEC, Observatoire de Paris, Section de Meudon, F-92195 Meudon, France
[2] Instituto de Fisica, UFRGS, C.P. 15051, Av. Bento Gonçalvès, 9500 Porto Alegre, RS-91500, Brazil

Received August 16, accepted November 28, 1988

Summary. We make a comparative study of the near-infrared Na I doublet and the Ca II triplet, among sets of stars, star clusters and galaxy nuclei. In particular, we study the semistellar nucleus of M31. We find evidence that the enhancement of the absorption feature around 8200 Å in galaxy nuclei is not due to a strengthening of the Na I lines, but rather to another absorber, possibly a molecular band at $\lambda \sim 8205$ Å which varies strongly with $\theta_{\rm eff}$ and metallicity. Therefore, an alternative explanation to the classical discussion about dwarf/giant star content in M31, is that of an increased metallicity in the semi-stellar nucleus of M31, with respect to its bulge or to the nucleus of M32. A similar result is found from molecular bands in the visible part of the spectrum, like CN and C_2 which show highly non-linear dependences on the metallicity.

Key words: stars: abundances – lines: identification – galaxies: stellar content of – clusters: open, and associations – clusters: globular

1. Introduction

The question of whether or not the stellar luminosity function in galaxy nuclei is dwarf-enriched has been discussed for over a decade. Contradictory answers have been given, up to now, in part because the metallicity may play too an important role in these composite objects. However, the way from an observed strong-lined spectrum to its interpretation in terms of a super metal-rich population is not straightforward. The existence of super metal-rich stars in the central parts of galaxies has been a matter of debate since Spinrad and Taylor raised this possibility (1971). For a review and complete discussion see Frogel (1988).

To probe the presence of a dwarf-enriched population the gravity discriminator Na I 8183, 8195 Å lines were considered in the analysis of M31 and M32: they led to discrepant results (Cohen, 1978; Faber and French, 1980). The conclusion of a dwarf-enriched population in M31 (Faber and French, 1980) was in contradiction with the observation of the FeH Wing-Ford band, at $\lambda \simeq 9910$ Å, a well known indicator of the presence of giant stars (Whitford, 1977), and with the observed strengths of CO and H_2O between 2 and 2.4 μm (Persson et al., 1980).

More recently, Jones et al. (1984) used the infrared Ca II triplet (8498, 8542 and 8662 Å) to investigate again this problem and concluded, in agreement with Cohen (1978) and Persson et al. (1980) that the luminosity function in the centre of M31 is not dwarf-enriched and that, rather, the near infrared light from this object is giant-dominated. Following this piece of work, Carter et al. (1986) initiated a similar study, considering both Na I and Ca II lines in the infrared. They confirmed a dwarf-enriched population in their galaxy nuclei sample, although their FeH measurements did not allow a large fraction of the mass to be contributed from cool dwarf stars: a very confusing situation, then. The controversy was reopened by Frogel (1988). He pointed out that the conclusions reached by Carter et al. (1986) would imply far too blue colours for elliptical galaxies which are else observed to be quite red objects.

We have recently developed a new method for population synthesis in galaxy nuclei, based on a library of integrated star cluster spectra exclusively (Bica and Alloin, 1986, 1987a, 1987b; Bica, 1988). In the course of this study, we have collected large data sets on star clusters and galaxy nuclei, but also on individual stars. Therefore, we can make a comparative analysis of the Ca II triplet and Na I doublet in these various objects, investigating more thoroughly their possible use as gravity, temperature or metallicity indicators. We think it might be enlightening to analyze the behaviour of Na I and Ca II lines in star clusters, before studying galaxy nuclei. These are simpler objects, for most of which the duration of star formation is negligible with respect to their age and are, hence, more easy to understand. We briefly present the data sets in Sect. 2. In Sect. 3, we provide a documented discussion of the dependences of Na I and Ca II lines on g, $\theta_{\rm eff}$ and $[Z/Z_\odot]$. Finally, this approach has been quantified in Sect. 4, while our concluding remarks are given in Sect. 5.

2. Observations

2.1. Set of stars

The sample of 62 stars studied by Jones et al. (1984) has been almost entirely reobserved, implemented with some new entries,

Send offprint requests to: D. Alloin

* Based upon observations collected at the European Southern Observatory (La Silla) and at Observatoire de Haute Provence (CNRS).

in order to get two independently atmosphere-corrected data sets, allowing to better track atmospheric H_2O residuals in the Na I region. The same instrumentation was used; a Boller and Chivens spectrograph equipped with a Reticon, at the 1.5 m European Southern Observatory (ESO) telescope, providing a spectral resolution of about 3 Å. The stars, together with updated physical parameters, $\theta_{\rm eff}$ ($\theta_{\rm eff} = 5040/T_{\rm eff}$), [Fe/H], $\log g$ are listed in Table 1.

2.2. *Star clusters and galaxy nuclei*

The near-infrared integrated spectra of star clusters and spectra of galaxy nuclei, considered in this paper, were collected at the 2.2 m ESO telescope, using a CCD detector, with a 10 Å spectral resolution. Detailed analysis of this data set is given in Bica and Alloin (1987a). The groups of star clusters and the spectral groups of galaxy nuclei are listed in Tables 2 and 3 respectively, together with some related physical parameters.

2.3. *M31 and M32 data*

The central regions in M31 and M32 were observed in August 1987 at the Haute Provence Observatory (OHP) 1.93 m telescope, with the Carelec spectrograph and a CCD detector. The resulting spectral resolution was 17 Å. The sky probe for M31 was taken from a separate frame, outside the galaxy body. Details on the observations, as well as a population synthesis over the visible and near-infrared ranges using a grid of star cluster W_λ as a function of age and metallicity are given elsewhere (Bica et al., 1989). We emphasize that data on the semi-stellar nucleus and bulge of M31 come from the same frame, owing to the use of a long slit. The innermost rows ($r < 4''$) corresponding to the central luminosity peak were summed up to represent the semi-stellar nucleus, while the bulge spectrum corresponds to the region at radius r from 4″ to 140″ on each side of the semistellar nucleus.

2.4. *Fringe corrections and atmospheric band cancellations*

A thorough discussion on fringe corrections is given in Bica and Alloin (1987a) regarding data collected at ESO for star clusters and galaxy nuclei. The fringe residuals were reduced down to the level of the data noise. In the case of OHP data (M31 and M32) fringes were eliminated through a classical flat-field correction. Stellar reticon data are, of course, not affected by this problem.

Table 1. Stellar data

	HD	m_v	Type	[Fe/H]	$\theta_{\rm eff}$	$\log g$	$W_{\rm FF}$(Na I)	W (CaT)
	1461	6.46	G0 V	+0.43	0.91	(4.45)	0.5	7.4
	2490	5.43	*M0 III	+0.3	1.38	(1.2)	0.4	10.0
	3443	5.57	G8 V	−0.16	0.93	4.57	0.4	6.6
	3651	5.87	K0 V	−0.17	1.0	4.5	0.6	7.4
	4656		K5 III			(2.4)	0.35	9.2
	4813	5.19	F7 IV/V	+0.03	0.84	(4.0)	0.25	6.2
	5133	7.2	K3 V			(4.5)	0.6	6.7
+	5780	7.61	K5 II/III	−0.5	1.31	(1.1)	0.35	7.9
	6482		K0 III			(2.4)	0.35	7.9
	7788	5.0	*F6 IV			(4.1)	0.3	6.5
	10380	4.44	K3 III	−0.30	1.26	1.5	0.5	9.1
	10700	3.50	G8 V	−0.34	0.94	4.6	0.4	6.1
	13611	4.37	*G6 II	0.0	0.98	3.0	0.45	8.7
	16160	5.8	K3 V	−0.01	1.06	(4.5)	0.8	7.3
	16234	5.68	*F7 V	−0.49	0.85	3.95	0.35	6.0
	16417	5.79	G5 IV	−0.20	0.86	4.4	0.35	7.2
	20010	3.8	*F8 V			(4.3)	0.15	6.1
+	20630	4.83	G5 V	+0.2	0.87	4.4	0.35	7.2
	20644		*K2 II/III			(1.9)	0.5	11.1
	20766	5.54	*G3/5 V	−0.10	0.86	4.5	0.4	6.3
	20794	4.27	*G8 III	−0.34	0.92	4.45	0.4	6.7
	20807	5.24	*G2 V	−0.20	0.87	4.5	0.45	6.3
	20894	5.52	*G6 II	−0.20	0.99	3.10	0.35	8.4
	22049	3.73	K2 V	−0.25	1.0	4.5	0.55	7.0
	22879	6.68	F9 V	−0.57	0.89	(4.1)	0.7	5.2
	23249	3.54	K0 IV	−0.07	1.02	3.73	0.4	7.1
+	26462	5.72	F4 V			(4.3)	0.4	6.8
	26965	4.43	K1 V	+0.01	1.08	(4.5)	0.35	7.0
	27371	3.65	*K0 III	+0.04	1.0	2.7	0.4	8.9
	27383	6.85	F9 V	< +0.23	0.84	4.3	0.3	8.0

Table 1 (continued)

HD	m_v	Type	[Fe/H]	θ_{eff}	log g	W_{FF}(Na I)	W(CaT)
27561	6.61	F5 V	−0.05	0.75	4.2	0.4	6.8
27697	3.76	*K0 III	−0.05	1.02	2.5	0.35	9.1
28305	3.53	K0 III	+0.15	1.03	2.7	0.25	9.3
29139	0.85	K5 III	−0.10	1.30	1.2	0.8	9.7
30652	3.19	F6 V	+0.15	0.79	4.45	0.3	6.4
32147	6.22	K3 V	+0.02	1.06	4.45	1.2	8.0
+ 32923	4.92	G4 V	−0.20	0.88	3.9	0.5	6.6
33256	5.12	F2 V	−0.60	0.82	4.18	0.25	6.0
37763	5.19	*K2 III	+0.35	1.05	2.8	0.55	8.2
38393	3.60	F6 V	−0.07	0.89	(4.1)	0.45	6.3
39364	3.81	*G8 III	−0.36	1.15	(3.0)	0.2	7.1
39801	0.80	*M2 lab		1.46	(0.7)	1.0	13.8
39853	3.66	*K5 III			(2.4)	0.4	8.3
40136	3.71	F1 III?	−0.20	0.68	4.00	0.4	6.2
41312	5.04	*K3 III	−0.60	1.26	0.9	−0.05	8.2
42581	8.14	M1 V		1.38	(4.8)	2.7	5.4
44213		M3 Ib/II			(0.9)	0.85	10.9
47205	3.96	K1 III	+0.07	1.02	3.08	0.45	7.5
202560	6.68	M0 V	0.0	1.31	4.56	1.85	5.5
+204139	5.78	K5 III			(2.4)	0.3	10.5
204867	2.89	G0 Ib	+0.09	0.92	1.4	0.7	12.7
+206453	4.73	G8 III			(3.0)	0.45	7.6
+206690	6.45	K1 III			(2.0)	0.45	12.8
+209688	4.46	K3 III			(1.0)	0.50	10.2
209750	2.93	G2 Ib	+0.14	0.97	1.4	0.6	13.0
212943	4.8	*K0 III			(3.0)	0.5	7.2
217357	7.89	M1 V	0.0	1.32	(4.8)	1.8	6.5
217364		G8/K0 III			(2.4)	0.35	7.3
218329	4.5	M1 III			(1.4)	0.50	10.7
219576	5.04	*M3 III			(1.4)	0.1	10.4
221146	7.10	dG0			(4.5)	0.05	7.7
221148		K3 III	0.07	1.07	2.6	0.55	8.1
221615	5.34	*M5 III			(1.4)	−0.4	10.7

Notes to Table 1:

+ New star with respect to Jones et al. (1984).

* Value of physical parameters improved with respect to Jones et al. (1984): from Bright Star Catalogue (Fourth Edition) or from Catalogue of stars observed photoelectrically, Jaschek et al., 1972).

Bracketted log g: the value has been derived from the general correlation log g, luminosity class.

All spectra were corrected for atmospheric absorption bands using hot stars (B2 to A0 spectral types, III to IV luminosity classes) as described in Bica and Alloin (1987a). With this method, the strong atmospheric H_2O band heads in the regions 7200 Å and 9300 Å cancel out and a control of their residuals provides a quality estimate of the weak H_2O head correction near the Na I lines: the expected residual is less than 0.2 Å.

3. Comparative spectral analysis

We illustrate in Fig. 1, for individual stars, the effect of gravity on the Na I and Ca II lines, at nearly constant effective temperature (spectral class M1 to M2). The Na I lines are much stronger in the dwarf star than in the giant and supergiant ones. In these latter two stars, the second Na I line at 8195 Å appears to be blended on its red wing with another absorber m of similar strength, at around 8205 Å. On the contrary, the Ca II triplet is enhanced in the giant and supergiant stars. These conclusions are in full agreement with previous studies (e.g. Cohen, 1978; Faber and French, 1980; Jones et al. 1984; Carter et al., 1986; Diaz et al., 1989). Notice also, the strengthening of the absorber m, redwards of Na I λ 8195, when gravity lowers.

We show in Fig. 2 the influence of effective temperature (T_{eff}) changes, at constant gravity corresponding to that of giant stars.

Table 2. Mean physical parameters and line-indices measurements for star cluster groups

Star cluster group	$\langle [Z/Z_\odot] \rangle$	$\langle$age$\rangle$ (10^7 yr)	W(CaT) raw	W(CaT) corr.	W_{FF}(Na I)	W_{BA}(Na I) # 74
Y1	−0.25	0.8	13.5	13.5	0.01	1.8
Y2	−0.4	2.7	13.8	9.7	−0.11	2.1
Y3A	−0.5	8.6	12.1	8.5	0.07	0.9
Y3B	−0.14	20	11.4	8.0	0.60	1.8
Y4	−1.1	50	10.3	7.2	0.7	1.3
I1	−0.02	120	11.4	8.0	1.0	1.7
I2	−0.9	250	11.2	9.5	0.1	1.35
G1	0.0	1650	11.0	11.0	0.4	2.0
G2	−0.25	1650	10.0	10.0	0.4	1.7
G3	−0.9	1650	8.7	8.7	0.3	1.0
G4	−1.45	1650	7.4	7.4	0.3	1.3
G5	−1.8	1650	5.0	5.0	0.2	0.5

Note: We recall the composition of star cluster groups, Y1(NGC 2004), Y2 (NGC 1847 and 2157), Y3A (NGC 1866), Y3B (NGC 1831, 1856 and 6705), Y4 (NGC 1868), I1 (NGC 2660), I2 (NGC 1783 and 1978), G1 (NGC 6440 and 6528), G2 (NGC 5927, 6316, 6356, 6388 and 6624), G3 (NGC 6638, 6652, 6715 and 6864), G4 (NGC 6093, 6453 and 6642), G5 (NGC 5024, 5824, and 6293).

Table 3. Spectral groups for galaxy nuclei, line equivalent widths and maximum metallicity attained in the population synthesis (see Bica, 1988 for details about the composition of groups and the population synthesis)

Spectral group	Prototype NGC	$[Z/Z_\odot]_{max}$	W(CaT)	W_{FF}(Na I)	W_{BA}(Na I) # 74
E1	4472	+0.6	11.0	0.7	2.5
E2	3115	+0.3	10.5	0.5	2.2
E3	4033	0.0	12.0	0.3	2.2
E4	4476	−0.5	11.0	0.25	1.5
E5	6861	+0.6	11.0	0.5	2.0
E6	5061	+0.3	11.2	0.6	2.0
E7	2865	+0.3	11.5	0.4	2.0
E8	5102	−0.5	11.2	0.0	1.7
S1	7049	+0.6	11.0	0.8	2.0
S2	1350	+0.3	9.5	0.4	1.7
S3	3521	+0.3	10.8	0.3	1.8
S4	3887	0.0	11.2	0.4	2.6
S5	2997	0.0	11.5	0.2	1.9
S7	5236	0.0	11.5	0.2	1.2
M32	nucleus	0.0	12.0	0.1	2.2
M31	semi-stellar nucleus	0.6	12.0	1.0	5.3
M31	bulge	0.3	11.5	1.1	2.8

The growing importance of molecular absorptions as T_{eff} decreases is striking. For spectral types M3 and M5, the feature *m*, at λ8205 has become much stronger than Na I λ8195, as does also the TiO band head at $\lambda > 8405$ Å which disturbs notably the Ca II triplet figure.

In Fig. 3, we have displayed a metallicity sequence for Galactic globular clusters. The groups G1 to G5, defined in Bica (1988), are labelled with their respective average metallicity. Group G1 includes the very strong-lined inner bulge globular clusters as NGC 6528 which are suspected to have $[Z/Z_\odot]$ as large as 0.2: these exhibit integrated spectra similar to those of massive galaxy nuclei in terms of metallic feature strengths. Globular clusters usually called metal-rich in the literature, like 47 Tuc, pertain in fact to group G2. Finally, very metal-poor

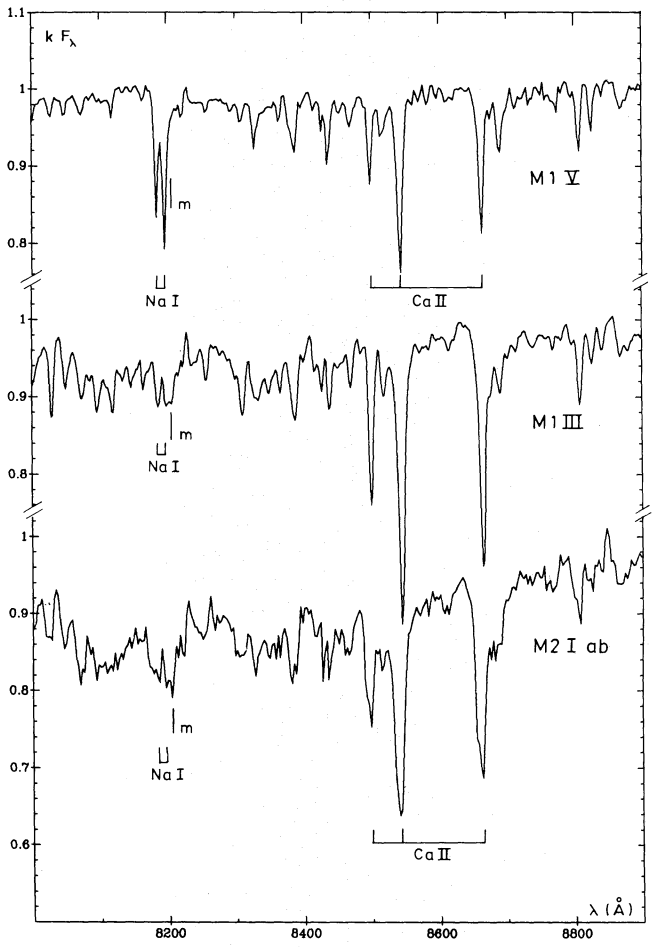

Fig. 1. A comparison of the near infrared spectra for stars of different surface gravity (spectral type M1-M2). This shows the gravity dependence of both Na I (enhanced in dwarf stars) and Ca II (enhanced in giant and supergiant stars). It also shows the contribution of a feature at 8205 Å approximately, which is not to be confused with Na I

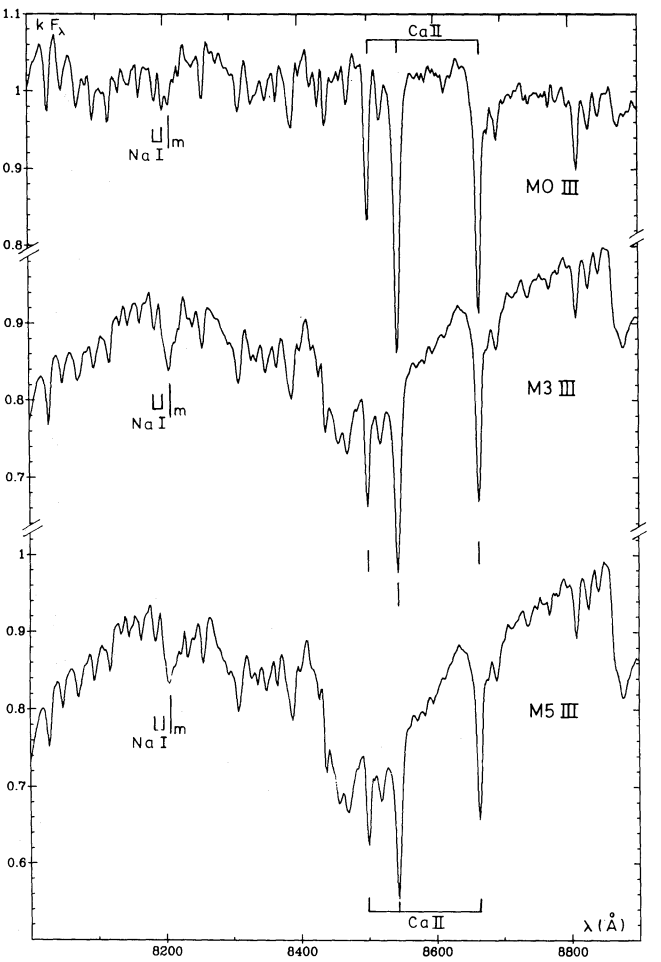

Fig. 2. In the same range, comparison of the spectra for giant stars of different effective temperatures. This demonstrates the increasing importance with $T_{\rm eff}$ of the TiO band around Ca II, and also of a feature *m*, redwards of Na I 8195 Å, at about 8205 Å

globular clusters, M15 for example, are in group G5. This sequence demonstrates essentially the metallicity effects on the Na I and Ca II lines, for a typical giant plus dwarf star mixture representing old populations. The evolution of the 8200 Å feature along the metallicity sequence, particularly the comparison between G2 and G1 shows that it is the absorption feature *m* in the red wing and *not the Na I lines*, that is strongly enhanced when the metallicity increases. This sequence of globular clusters also shows that, when a large metallicity range (2 dex) is considered, the influence of the metallicity on the Ca II triplet lines, becomes conspicuous. In the analysis performed by Jones et al. (1984), a narrower metallicity range was considered in the star sample and then, the Ca II triplet displayed only its strong dependence on gravity (see also Fig. 1). However, the Ca II triplet dependence on metallicity might be more relevant for stellar population synthesis in galaxy nuclei, as suggested by integrated spectra analysis (Bica, 1988).

We provide in Fig. 4a the integrated spectrum in the Na I, Ca II wavelength range, when a young age component (10^7 yr) is present. Indeed, NGC 2004 is an LMC cluster at the red supergiant phase (Bica and Alloin, 1986, 1987a); the presence of supergiants enhances considerably the Ca II triplet while the Na I lines and the suspected molecular feature *m*, at λ8205, are of equal strength. Similarly, Fig. 4b shows the integrated spectrum when an important contribution of hot stars occurs. This spectrum is an average of blue LMC cluster spectra, blue galaxy nucleus spectra and one Galactic open cluster spectrum. The Paschen lines become prominent and must contaminate considerably the Ca II lines. Let us note however that, in the case of a burst superimposed on an old population, a phase like the red supergiant one would simply produce a slight enhancement of the Ca II feature with respect to its normal intensity in a typical giant plus dwarf mixture occurring in an old population with a metallicity equal to that of the burst. In composite populations the Ca II lines will always be affected by *dilution* due to older stellar components. Hence, the star-forming activity in a galaxy nucleus will not be recognized through Ca II triplet supergiant phase signature, as easily as in the case of an isolated star cluster.

Last, we compare in Fig. 5, the spectra of M31 (semistellar nucleus and bulge), M32 and an average of 32 red strong-lined galaxy nuclei (Bica and Alloin, 1987b). The semistellar nucleus in M31 exhibits a strong increase of the absorption feature around

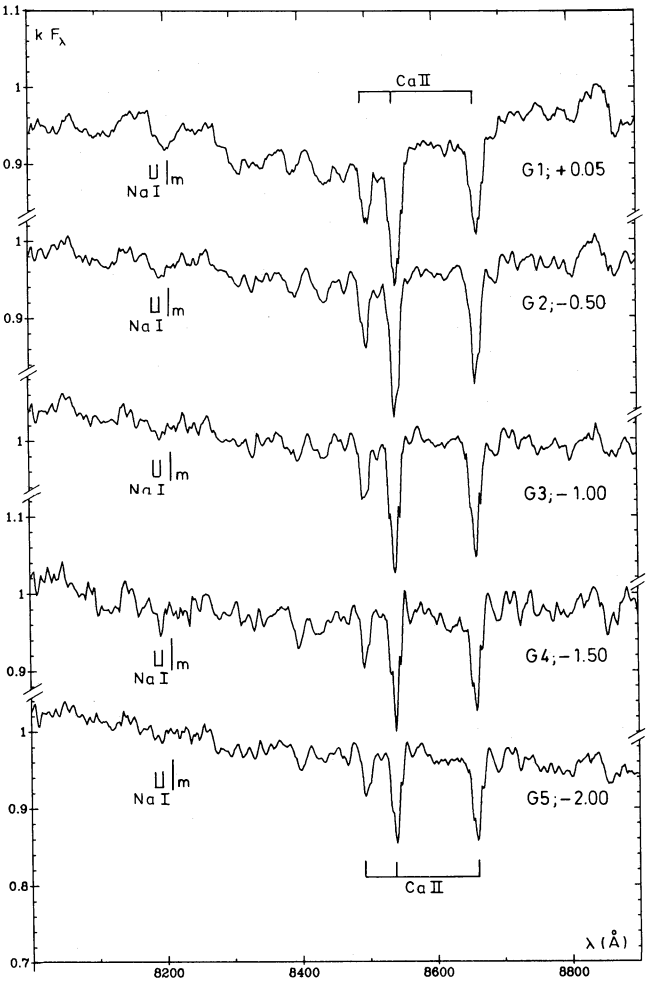

Fig. 3. A metallicity sequence of integrated globular cluster spectra. The composition of the various groups is recalled in Table 2. This figure illustrates the metallicity dependence of Na I and Ca II lines

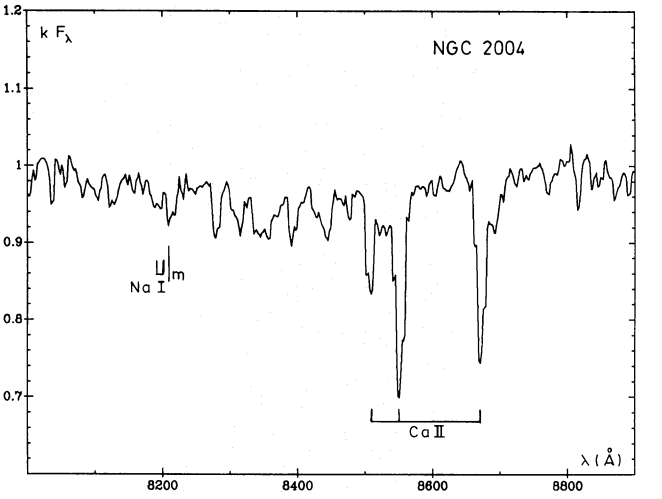

Fig. 4a. Spectrum of a young star cluster, at the red supergiant phase (NGC 2004), showing enhanced Ca II

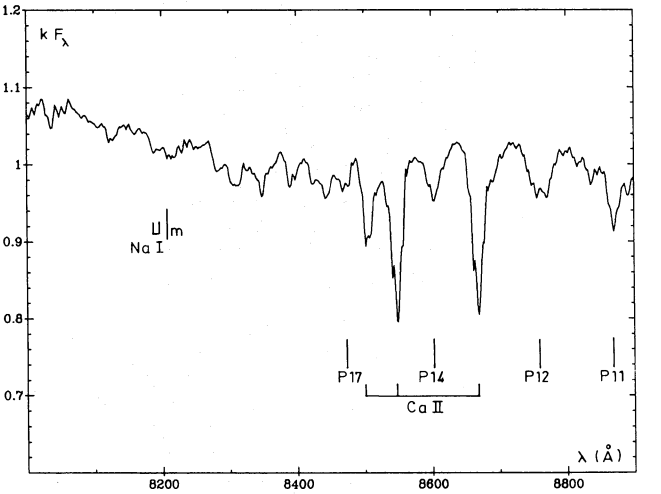

Fig. 4b. Mean spectrum for young blue star clusters and blue galaxy nuclei: Paschen lines become prominent

8200 Å, with respect to the bulge of M31 and to the nucleus of M32. A careful analysis shows that it is the molecular feature *m*, at λ8205 rather than the Na I lines, which is responsible for this strengthening. In the average spectrum of 32 strong-lined galaxy nuclei, the absorption at 8200 Å, is symmetric around this wavelength, suggesting an equal contribution from the Na I lines (8183 and 8195 Å) and the molecular feature *m*, redwards of 8205 Å, just as in the strong-lined globular cluster group G1 (Fig. 3). Let us note however that, for these 32 southern Shapley-Ames galaxies, the spectrograph slit includes a larger volume than in M31, so that possibly strong-lined regions equivalent to the semistellar nucleus of M31 are diluted in the surrounding bulge contribution. This may explain the fact that in the average red strong-lined galaxy nuclei, the absorption at 8200 Å, with respect to the Ca II triplet, is not as strong as in the semistellar nucleus of M31 but rather looks like in the M31 bulge. Figure 5 also indicates that the 8200 Å feature remains constant throughout the bulge of M31, at least up to a radius of 140″.

We compare in Table 4, the observed equivalent widths W_λ of metallic features for M31, M32 (Bica et al., 1989) and for spectral groups of red nuclei (Bica, 1988). These values have been used for population synthesizing M31 and M32, as well as the group of galaxy nuclei, through a new method based on a grid of star cluster metallic features and Balmer lines, as a function of age and metallicity. We recall in Table 4 the observed W_λ of some of the metallic features considered for the computation, and the maximum metallicity $[Z/Z_\odot]_{max}$ reached up in the synthesis. One can recognize the large dynamical range of CNλ4216, and to a lesser extent of Mg I + MgH, as a function of metallicity, with respect to other features. This differential behaviour of metallic features in integrated spectra of star clusters and galaxy nuclei, has been analyzed in detail in Bica and Alloin (1986, 1987b). Synthetic spectra computations of molecular features, C_2 and MgH, in the region 5000, 5200 Å, also indicate such strong metallicity dependences (Barbuy, 1988, private communication). We suggest that the enhancement of the absorption feature *m*, at λ8205, results too from a strong metallicity dependence, and that the semi-stellar nucleus in M31 is indeed extremely metal-rich.

We have just seen that, redwards of the Na I lines, appears an absorption feature, especially in late giant stars, at ~8205 Å. Its

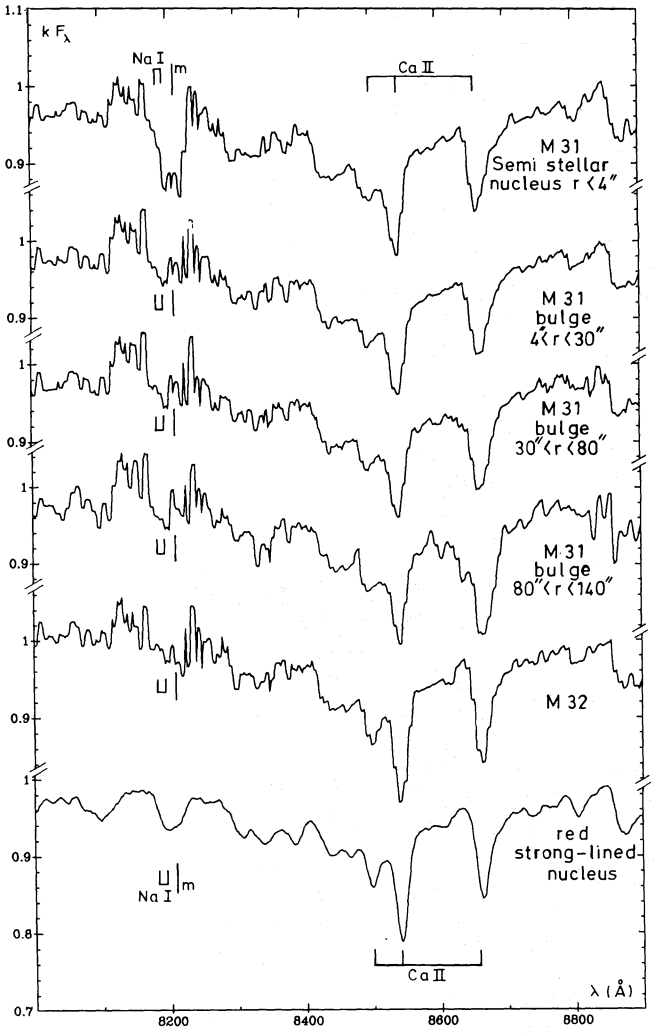

Fig. 5. Comparative display of the spectra for: (a) the semi-stellar nucleus in M31; (b), (c), (d) the bulge in M31, at 3 different radii; (e) the nucleus in M32; (f) a mean of 32 strong-lined red galaxy nuclei

strength depends both on the effective temperature of the star and on metallicity. What about its identification? It is well known that many TiO lines are to be found in this spectral region, and indeed, from model calculation, there appears to be a TiO band head at 8205.5 Å (Boyer and Sotirovski, 1988, private communication). Their computation was performed for conditions encountered in solar sunspots and therefore, the relative strengths of TiO bands may not be representative of what occurs in a late giant. However, this TiO band with head at 8205 Å is a possible identification. It was also detected in the spectrum of βPeg, an M2 giant star (Davis, 1947), at 8205.8 Å (TiO γ(0.2) a-head). Else, we do not find any evidence for the existence of a TiO band head at 8194 Å, neither in the spectrum of βPeg, nor in the atlas of TiO bands (there are isolated TiO lines around, but no band-head). Other molecular absorbers should be checked for identification in this region, in particular molecules like CN and C_2 which are known to be quite sensitive to metallicity.

4. Comparative analysis using indices

4.1. The Na I measurements

We have first adopted the same convention as Faber and French (1980) for measuring the Na I 8183 Å, 8195 Å absorption, by a choice of continuum points at $\lambda \sim 8170$ Å and $\lambda \sim 8210$ Å. The results W_{FF} (Na I) are given in Tables 1, 2, 3 for stars, star clusters and galaxy nuclei respectively. The measurements shown in Fig. 6 for stars, are consistent with the relationship previously found by Faber and French (1980).

This procedure is however extremely sensitive to the nearby molecular absorption *m* which appears in late-type stars, redwards of 8205 Å. In particular, for late type giant and supergiant stars, where the Na I lines are weak indeed, this definition of W_{FF}(Na I) results in an artificial Na I emission. This method works out well for distinguishing types of individual stars. However, it is practically impossible to use this indice as a gravity indicator in composite objects like star clusters or galaxy nuclei: the actual blend with the molecular feature *m* prevents an accurate measurement of Na I lines.

Table 4. Metallicity dependence of various features in the visible and near-infrared regions

	Ca II K 3933 Å	W_λ(Å)					$[Z/Z_\odot]_{max}$
		CN 4216 Å	G-band 4300 Å	Mg+MgH 5170 Å	Ca II (2) 8542 Å	Ca II (3) 8662 Å	
M31 semi-stellar nucleus	19.0	14.4	9.0	10.1	7.2	6.3	0.6
M31 bulge	17.6	11.5	9.2	9.3	6.8	6.4	0.3
M32	17.5	8.4	8.8	7.0	6.8	5.5	0.0
S1	19.0	13.0	10.0	9.8	5.6	4.6	0.6
E1	16.8	14.5	9.3	10.3	6.1	4.9	0.6
S2	16.4	10.4	8.8	9.2	5.9	4.6	0.3
E3	15.3	7.3	8.6	7.7	6.6	5.5	0.0
E4	13.7	3.4	6.8	6.3	5.2	4.7	−0.5

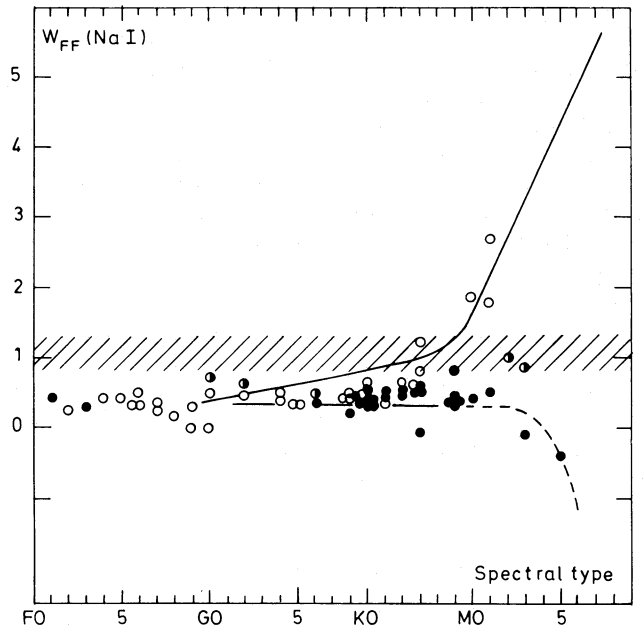

Fig. 6. W_{FF}(Na I) measured in the same way as Faber and French (1980), for our sample stars. Black dots are giant stars, half-filled circles are supergiants and open circles represent dwarf stars. Continuous lines reproduce the relationship found by Faber and French (1980) and the hatched area indicate the W_{FF}(Na I) range in M31 (semi-stellar nucleus and bulge)

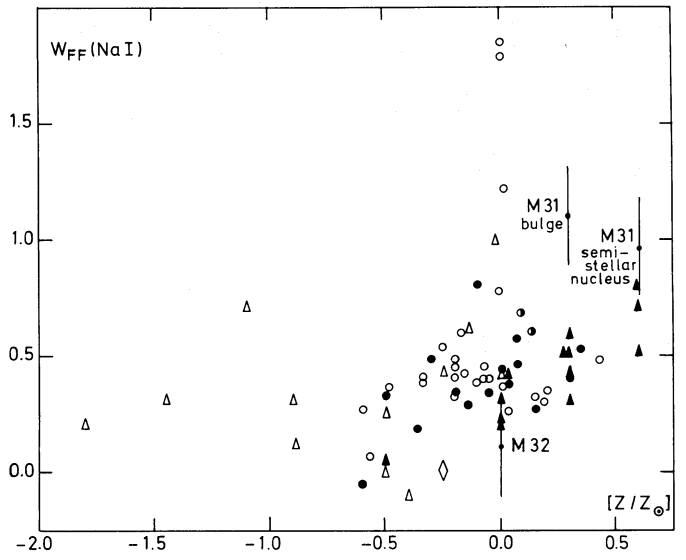

Fig. 7. W_{FF}(Na I), as a function of metallicity $[Z/Z_\odot]$. We recall that we use $[Z/Z_\odot] \simeq$ [Fe/H] all throughout this paper. Star cluster groups are defined in Table 2 and spectral groups of galaxy nuclei in Table 3. The metallicity value attached to each spectral group of galaxy nuclei is the maximum metallicity obtained in the stellar population synthesis (Bica, 1988). Values for M31 and M32 are shown as small dots. Groups of galaxy nuclei are filled triangles; star clusters are empty triangles (except NGC 2004, an empty diamond). Black dots represent giant stars, half-filled circles supergiants and open circles dwarfs

We have displayed in Fig. 7, W_{FF}(Na I) for stars, star clusters and galaxy nuclei, as a function of metallicity. There appears to be a weak dependence with $[Z/Z_\odot]$, as expected. *Taking into account this metallicity trend, it is not required anymore for the M31 semistellar nucleus to contain a strong dwarf contribution.* We emphasize however that this measurement, owing to the definition of its local continuum, reflects the profile of the λ8200 feature rather than its depth. Hence, it is very dependent on the nearby molecular feature depth. The M31 bulge and semistellar nucleus give similar W_{FF}(Na I) (Fig. 7), although they differ considerably in feature strength (Fig. 5). For comparison, we also provide in Tables 2 and 3, W_{BA}(Na I, *m*) as defined in Bica and Alloin (1987a); this includes the whole absorption in the 8160–8234 Å window (# 74 in the original paper) and encompasses the total feature normally observed in the integrated spectra of composite objects, it is obviously a blend of Na I lines and the molecular feature at 8205 Å. As long as measurements are performed in the same way for star clusters and galaxy nuclei, it can be used in stellar population synthesis. However, its dependences on gravity (Na I lines), θ_{eff} (molecular feature) and metallicity (both features) make it less powerful.

4.2. *The Ca II measurements*

We have made Ca II measurements following Jones et al. (1984) which use continuum points so as to minimize the effects of velocity dispersion. These are shown in Tables 1, 2 and 3, where W(CaT) stands for the sum of the 3 lines. We provide in Fig. 8, the new relationship W(CaT) vs log g for our sample of stars within the metallicity range $-0.60 < [Fe/H] < +.40$. The dependence of W(CaT) on metallicity is displayed in Fig. 9. For individual stars, the Paschen lines contamination becomes prominent for spectral types earlier than F, which we have omitted. In the star cluster integrated spectra, Paschen line contamination is responsible for the large W(CaT) raw measurements provided in Table 2 (column (4)), for groups Y2 to I2 (ages from $2\ 10^7$ yr to $2\ 10^9$ yr). From isolated Paschen lines we have estimated the correction to be applied to Ca II lines: from 30% in groups Y2, Y3A, Y3B, Y4 and I1 to 15% in group I2 and null in the globular cluster groups G. It is this "net" W(CaT) absorption which is given in column (5) and displayed in Fig. 9. In the case of group Y1 (NGC 2004) at the red supergiant phase, the large W(CaT) is purely due to Ca II, as there is no sign of Paschen contribution: this increased value indeed reflects the presence of supergiant stars in NGC 2004.

The measurements for star clusters and galaxy nuclei are consistent with respect to velocity dispersion effects, as the former are instrumentally degraded to a 12 Å resolution. On the contrary, stars were observed at a 3 Å spectral resolution, so that the actual W(CaT) values for stars are upper limits, if compared to star clusters or galaxy nuclei. This point was raised by Carter et al. (1986) and Boulade and Vigroux (1988, private communication). A quantitative estimate of the effect is still presently difficult to perform.

In conclusion, we find that W(CaT) is also metallicity dependent, although not as much as other metallic or molecular features (CN or Mg+MgH, in Table 4). Figure 9 allows to compare the metallicity and gravity effects. It suggests that, when metallicity effects are taken into account, star cluster and galaxy nuclei integrated spectra have a more important contribution from giant starlight than from dwarf starlight in the near infrared.

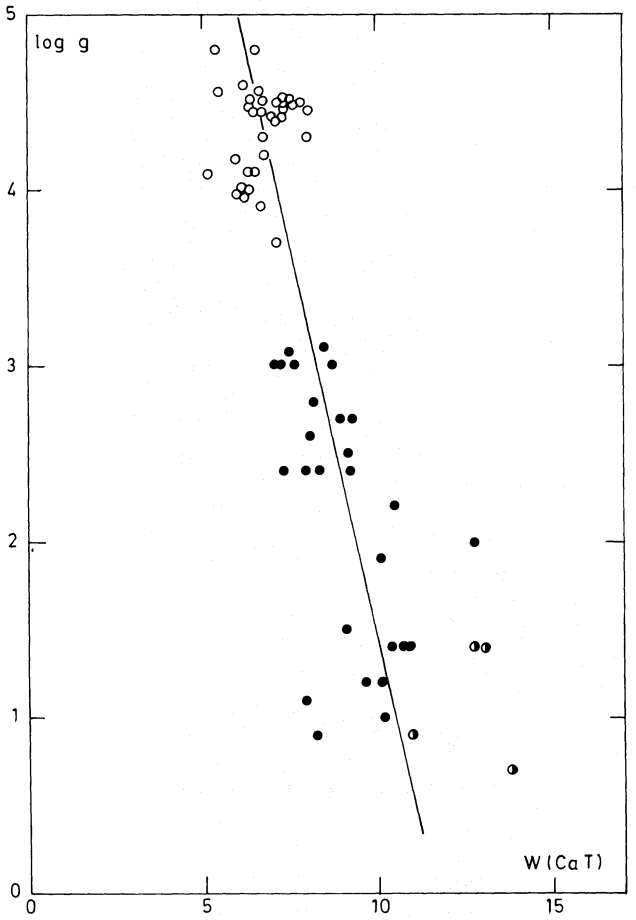

Fig. 8. An improved log g versus W(CaT) relationship from stellar data. Symbols as in Fig. 7

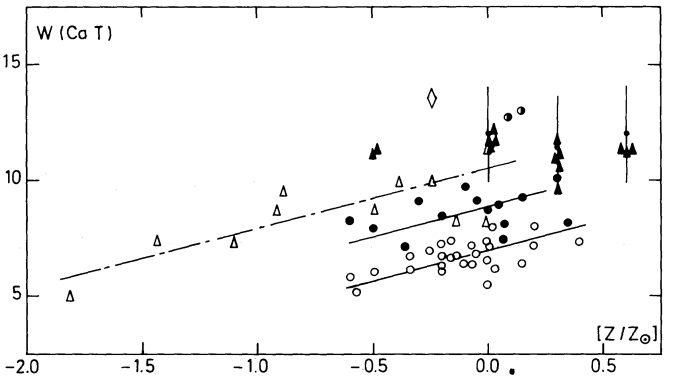

Fig. 9. W(CaT) as a function of metallicity. Same symbols and comments as in Fig. 7. We have omitted F stars and we have corrected star cluster measurements for the Paschen line contribution. Same symbols as in Fig. 7

5. Concluding remarks

1. We find that the absorption around 8200 Å is from the Na I 8183 and 8195 Å lines *and from another feature at 8205 Å which becomes prominent in giant stars cooler than M1.* It is possibly a molecular band of TiO with head at 8205 Å. The strength of this feature is strongly dependent on stellar temperature and metallicity.

2. We confirm that the Na I and Ca II lines are indicators of gravity. They also depend on metallicity. This last property may be of a major issue in galaxy nuclei analysis. The Na I and Ca II metallicity dependence is however less pronounced than that of other features like CN or Mg + MgH, in the visible range.

3. We observe in the spectrum of the semistellar nucleus in M31 (4″ in radius) an enhanced absorption in the 8200 Å region: it is due to the 8205 Å feature, not to Na I. We conclude that all gravity sensitive features in the near infrared, Na I, Ca II, FeH, CO, H_2O point towards giant-dominated light in this object. We find also a metallicity increase in the semistellar nucleus with respect to the bulge in M31. These conclusions are in agreement with Cohen (1978) early findings.

4. In the mean high signal to noise ratio spectrum of a red-lined galaxy nucleus, the absorption around 8200 Å is as well largely contributed by the 8205 Å band. An exceptional dwarf-enriched stellar luminosity function is no more required in such galaxy nuclei.

Acknowledgements. E.B. acknowledges a fellowship from the Brazilian Institution CNPq. We are grateful to the staff at ESO (La Silla and Garching) and Haute Provence Observatory, for assistance at various stages of this work. We are deeply indebted to Dr. Pelat who obtained some of the stellar data for this study.

References

Bica, E., Alloin, D.: 1986, *Astron. Astrophys.* **162**, 21
Bica, E., Alloin, D.: 1987a, *Astron. Astrophys.* **186**, 49
Bica, E., Alloin, D.: 1987b, *Astron. Astrophys. Suppl. Ser.* **70**, 281
Bica, E.: 1988, *Astron. Astrophys.* **195**, 76
Bica, E., Alloin, D., Schmidt, A.: 1989, *Monthly Notices Roy. Astron. Soc.* (in press)
Carter, D., Visvanathan, N., Pickles, A.: 1986, *Astrophys. J.* **311**, 637
Cohen, J.: 1978, *Astrophys. J.* **221**, 788
Davis, D.: 1947, *Astrophys. J.* **106**, 28
Diaz, A., Terlevich, E., Terlevich, R.: 1989, *Monthly Notices Roy. Astron. Soc.* (in press)
Faber, S., French, H.: 1980, *Astrophys. J.* **235**, 405
Frogel, J.: 1988, *Ann. Review of Astron. and Astrophys.* **26**, 51
Frogel, J.: 1988, in "Towards understanding galaxies at large redshifts", ed. R. Kron, A. Renzini, Kluwer, p. 1
Jaschek, C., Hernandez, E., Sierra, A., Gerhardt, A.: 1972, University of La Plata Publication
Jones, J., Alloin, D., Jones, B.: 1984, *Astrophys. J.* **283**, 457
Persson, S., Cohen, J., Sellgren, K., Mould, J., Frogel, J.: 1980, *Astrophys. J.* **240**, 779
Spinrad, H., Taylor, B.: 1971, *Astrophys. J. Suppl.* **22**, 445
Whitford, A.: 1977, *Astrophys. J.* **211**, 527